Structural transformations in quasicrystals induced by higher-dimensional lattice transitions

(Article begins on next page)

11 May 2024

UNIVERSITÀ DEGLI STUDI DI TORINO

This is an author version of the contribution published on:

The definitive version is available at:

Structural transformations in quasicrystals induced by higher-dimensional lattice transitions

Giuliana Indelicato[1], Tom Keef[1], Paolo Cermelli[2], David G. Salthouse[1], Reidun Twarock[1], and Giovanni Zanzotto[3]

[1]York Centre for Complex Systems Analysis, Departments of Mathematics and Biology, University of York, UK.
[2]Dipartimento di Matematica, Università di Torino, Italy.
[3]Dipartimento di Metodi e Modelli Matematici per le Scienze Applicate, Università di Padova, Italy.

December 5, 2015

Abstract

We study the structural transformations induced, via the cut-and-project method, in quasicrystals and tilings by lattice transitions in higher dimensions, with a focus on transition paths preserving at least some symmetry in intermediate lattices. We discuss the effect of such transformations on planar aperiodic Penrose tilings, and on three-dimensional aperiodic Ammann tilings with icosahedral symmetry. We find that locally the transformations in the aperiodic structures occur through the mechanisms of tile splitting, tile flipping, and tile merger, and we investigate the origin of these local transformation mechanisms within the projection framework.

1 Introduction

Quasicrystals are aperiodic structures with long-range order that generate diffraction patterns with non-crystallographic symmetries. After earlier theoretical efforts for describing aperiodic structures, for instance in the works of Penrose (1978), de Bruijn (1981), and Mackay (1982), the experimental discovery of quasicrystals in AlMn alloys by Shechtman et al. (1984) spurred great interest, also in the mathematical community. A standard way of generating mathematical models for quasicrystal structures is by means of the 'cut-and-project' method (de Bruijn, 1981; Levitov and Rhyner, 1988; Katz, 1989; Kramer and Schlottmann, 1989; Baake et al., 1990a,b; Senechal, 1996): the points of the quasicrystal are obtained by projection, to a low-dimensional subspace, of suitably selected points of a higher dimensional

1

lattice. If the projection subspace is invariant with respect to a subgroup of the point group of the lattice, then the resulting quasicrystal has the same symmetry.

Cut-and-project quasicrystals give rise to aperiodic tilings of space or the plane, which are obtained from the aperiodic point sets through a general method known as the dualisation technique (Senechal, 1996). This provides a general procedure for the construction of aperiodic tilings with non-crystallographic symmetry, like icosahedral tilings of space.

We are interested in transformations of such tilings that preserve at least some symmetry, and to this end we consider higher dimensional analogs of the Bain-like strains, i.e. lattice deformations such that the intermediate configurations during the transition maintain a common (perhaps maximal) symmetry subgroup. Such strains are considered, for instance, in the investigation of the three-dimensional (3D) reconstructive martensitic phase transformations in crystalline substances (Bain, 1924; Wayman, 1964; Boyer, 1989; Toledano and Dmitriev, 1996; Christian, 2002; Pitteri and Zanzotto, 2002; Bhattacharya et al., 2004; Capillas et al., 2007). The basic observation is that, provided there exists some common symmetry subgroup of the higher dimensional lattices before and after transition, one can determine the corresponding higher dimensional Bain strains and induce, via projection, structural transformations in the associated quasicrystals and tilings, which preserve the intermediate symmetry if the projection subspace is also invariant under the common symmetry subgroup.

Fig. 1 gives a low-dimensional sketch of the proposed procedure: a 2D square lattice is deformed into a rhombic lattice by an affine deformation, the 2D analog of the Bain strain. The point sets (quasicrystals) change accordingly, and this in turn induces a transformation of the tilings in the projection subspace E through the formation of new tiles and the change of shape of the existing ones (cf. Sect. 3). Analogous effects occur in higher dimensions.

As a first application of our methods we study the transformations of the Penrose tiling of the plane into the tilings induced by the 5D face-centered cubic (FCC) and body-centered cubic (BCC) lattices, respectively, while keeping at least the five-fold symmetry at intermediate configurations. These quasicrystals are obtained by projection of the 5D lattices onto a plane invariant with respect to a suitable integral representation of the cyclic group C_5. One of these lattice paths in the higher dimensional space is obtained through the compression of the 5D hypercubic cell along a body diagonal, similarly to the rhombohedral strain relating simple cubic (SC) and BCC lattices in 3D (Pitteri and Zanzotto, 2002).

We find that, in projection, the classical Penrose rhomb tiling of the plane transforms into triangle tilings through three basic mechanisms, involving the flipping, bisection, and merger of tiles. These mechanisms result from, and indeed correspond to, changes in the geometry of the projection window
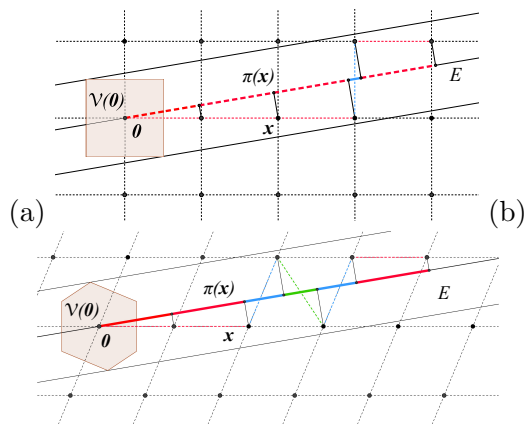
Figure 1: A 2D square lattice is deformed into a rhombic lattice by an affine deformation. The corresponding 1D quasicrystals are obtained by projecting onto the subspace E the lattice points that lie within the strip, whose width is determined by the Voronoi cell at the origin (shaded polygon - cf. Sect. 3). As a result of the lattice deformation, the Voronoi cell changes structure: new facets are created and this, in turn, induces the formation in the projection subspace E of new tiles and the change of shape of the existing ones. We notice that the Voronoi cell, whose facet structure determines the structure of the projected tiling, does not deform through the same affine deformation as the lattice. (a) Square lattice: the Voronoi cell is a square and only two tiles are present (dashed and continuous segments); (b) rhombic lattice: the Voronoi cell is an hexagon and there are three different types of tiles (dashed, dotted and continuous segments).

as a consequence of the deformation of the 5D lattice.

Fig. 2 illustrates these effects by showing the external shape of the projection windows (see Sect. 3) and the corresponding plane tilings along a symmetry-preserving transition path between the SC lattice in 5D (Penrose tiling) and the BCC lattice in 5D (triangle tiling). The projection windows are three dimensional, but it is indeed the structure of the projected 3D facets (not shown here) of the full 5D Voronoi cell that determines the shape and structure of the tilings. Further, the supplementary movie (FCC_Movie.avi) in the Supplementary Material shows how the projection window changes along a full transition path from a simple cubic lattice to a face-centered cubic lattice.

We also apply this technique to the study of the transformations of the 3D icosahedral quasicrystals and their associated tilings of space, obtained by projection of the SC and FCC lattices in 6D (Papadopolos et al., 1993, 1997, 1998; Niizeki, 2004), suggesting that the same mechanisms as above occur also in these 3D aperiodic structure transformations.
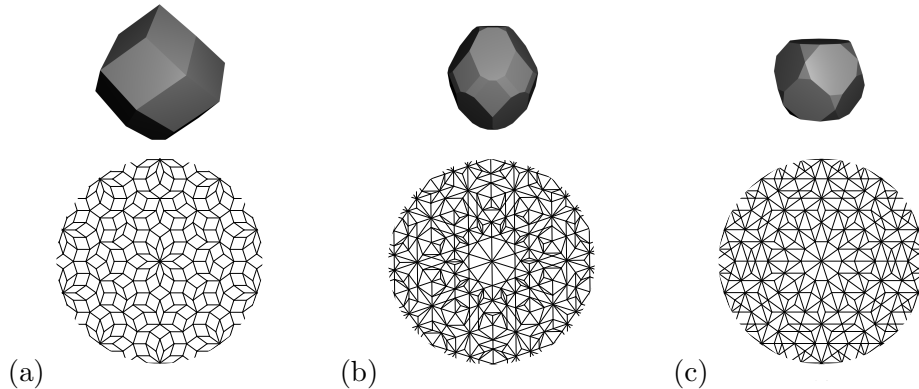
Figure 2: Three snapshots of the 3-dimensional projection window and the corresponding planar tiling along a 5-dimensional lattice transition preserving five-fold symmetry. (a) The projection window of the cubic lattice and the corresponding Penrose tiling; (b) an intermediate step; (c) the final step: the body-centered cubic lattice and the induced triangle tiling.

The approach presented here complements the work modelling experimentally observed transformations between crystalline and quasicrystalline structures (Toledano and Dmitriev, 1996; Tsai, 2008), which have been studied from a 6D viewpoint in the literature, see Sect. 4 for a discussion. In contrast, our main focus are the structural transformations of aperiodic structures such as plane or space tilings, or of other icosahedral assemblies in 3D relevant in the investigation of viral capsids (Keef and Twarock, 2009; Patera and Twarock, 2002; Twarock, 2004, 2006); our methods have indeed been applied in a recent study of the conformational changes in viruses with icosahedral symmetry (Indelicato et al., 2011).

2 Transition paths for lattices

Let $GL(n,\mathbb{Z})$ be the group of $n \times n$ unimodular integer matrices, $GL(n,\mathbb{R})$ the group of $n \times n$ invertible real matrices, $O(n)$ and $SO(n)$ the orthogonal and special orthogonal group of $\mathbb{R}^n$, and $Sym^+(n,\mathbb{R})$ the set of $n \times n$ symmetric positive definite matrices with real coefficients. For a basis $\{\boldsymbol{b}_\alpha\}_{\alpha=1,\dots,n}$ of $\mathbb{R}^n$, we write $B \in GL(n,\mathbb{R})$ for the matrix with column vectors $\boldsymbol{b}_\alpha$. We denote by

$$\mathcal{L}(B) = \{\boldsymbol{x} = \sum_{\alpha=1}^{n} m^\alpha \boldsymbol{b}_\alpha \,:\, m^\alpha \in \mathbb{Z}\}$$

the lattice with basis $\{\boldsymbol{b}_\alpha\}$. All other lattice bases have the form $\{\sum_{\beta=1}^n M_\alpha^\beta \boldsymbol{b}_\beta\}$, with $M_\alpha^\beta \in GL(n,\mathbb{Z})$. Moreover we write

$$\Lambda(B) = \left\{ M_\alpha^\beta \in GL(n,\mathbb{Z}) \ : \ \exists Q \in O(n) \text{ such that } Q\boldsymbol{b}_\alpha = \sum_{\beta=1}^n M_\alpha^\beta \boldsymbol{b}_\beta \right\},$$

for the *lattice group* of $\mathcal{L}(B)$, and

$$\mathcal{P}(B) = \left\{ Q \in O(n) \ : \ \exists M_\alpha^\beta \in GL(n,\mathbb{Z}) \text{ such that } Q\boldsymbol{b}_\alpha = \sum_{\beta=1}^n M_\alpha^\beta \boldsymbol{b}_\beta \right\},$$

for its *point group*. The following notations are equivalent:

$$Q\boldsymbol{b}_\alpha = \sum_{\beta=1}^n M_\alpha^\beta \boldsymbol{b}_\beta \qquad \Leftrightarrow \qquad QB = BM.$$

The point and lattice groups are related via the identity

$$\Lambda(B) = B^{-1}\mathcal{P}(B)B, \tag{1}$$

and moreover

$$\mathcal{P}(RB) = R\mathcal{P}(B)R^\top, \qquad \mathcal{P}(BM) = \mathcal{P}(B),$$
$$\Lambda(RB) = \Lambda(B), \qquad \Lambda(BM) = M^{-1}\Lambda(B)M,$$

for $R \in O(n)$ and $M \in GL(n,\mathbb{Z})$. We therefore will also write $\mathcal{P}(\mathcal{L})$ for the point group of the lattice $\mathcal{L}$.

A lattice basis is characterised (modulo rotations) by its *lattice metric*

$$C = B^\top B \in Sym^+(n,\mathbb{R}),$$

and the lattice group is the subgroup of $GL(n,\mathbb{Z})$ that fixes the metric (Pitteri and Zanzotto (2002)):

$$M \in GL(n,\mathbb{Z}), \quad M^\top CM = C \qquad \Leftrightarrow \qquad M \in \Lambda(B). \tag{2}$$

Important examples of n-dimensional lattices are the simple cubic (SC), body-centered cubic (BCC) and face-centered cubic (FCC) lattices, given by (see e.g. Levitov and Rhyner (1988)):

$$\mathcal{L}_{SC} = \{\boldsymbol{x} = (x_1,\ldots,x_n) \ : \ x_i \in \mathbb{Z}, i = 1,\ldots,n\},$$
$$\mathcal{L}_{BCC} = \{\boldsymbol{x} = \tfrac{1}{2}(x_1,\ldots,x_n) \ : \ x_i \in \mathbb{Z}, \ x_i = x_j \mod 2, i,j = 1,\ldots,n\},$$
$$\mathcal{L}_{FCC} = \left\{ \boldsymbol{x} = \tfrac{1}{2}(x_1,\ldots,x_n) : x_i \in \mathbb{Z}, \ \sum_{j=1}^n x_j = 0 \mod 2 \right\}. \tag{3}$$

A basis for the above SC lattice is the canonical basis. The point group of the simple cubic lattice is the so-called hyperoctahedral group

$$B_n = O(n) \cap GL(n, \mathbb{Z}).$$

While the point groups of the three cubic lattices in (3) coincide, their lattice groups do not. Indeed, they are integral representations of the common point group which are non-conjugate in $GL(n, \mathbb{Z})$ (this is indeed the defining property for lattices with distinct Bravais types, see for instance Pitteri and Zanzotto (2002)).

For a matrix group $\mathcal{G} \subset GL(n, \mathbb{Z})$ we have the following standard definition:

Definition 2.1. *The centraliser $\mathcal{Z}(\mathcal{G}, \mathbb{R})$ of $\mathcal{G}$ in $GL(n, \mathbb{R})$ is the group*

$$\mathcal{Z}(\mathcal{G}, \mathbb{R}) = \left\{ N \in GL(n, \mathbb{R}) : N^{-1}GN = G, \quad \forall G \in \mathcal{G} \right\}.$$

The centraliser of $\mathcal{G}$ can be obtained by solving the linear equations $G_i C = C G_i$ in the unknown C, where G_i are generators of $\mathcal{G}$. Hence, the centralisers of a finitely generated group in general depend linearly on a finite list of real parameters.

We define a lattice transition as a continuous transformation between two lattices $\mathcal{L}_0$ and $\mathcal{L}_1$ along which some symmetry is preserved, described by a common subgroup $\tilde{\mathcal{G}} \subset GL(n, \mathbb{Z})$ of the lattice groups of the intermediate lattices.

Definition 2.2. *Let $\mathcal{L}_0$ and $\mathcal{L}_1$ be two lattices, and $\mathcal{G} \subset \mathcal{P}(\mathcal{L}_0)$. We say that there exists a transition between $\mathcal{L}_0$ and $\mathcal{L}_1$ with intermediate symmetry $\mathcal{G}$ if there exist bases B_0 and B_1 of $\mathcal{L}_0$ and $\mathcal{L}_1$, and a continuous path $B : [0, 1] \to GL(n, \mathbb{R})$, with $B(0) = B_0$ and $B(1) = B_1$, such that, for*

$$\tilde{\mathcal{G}} = B_0^{-1} \mathcal{G} B_0 \subset \Lambda(B_0),$$

one has

$$\tilde{\mathcal{G}} \subset \Lambda(B(t)), \qquad t \in [0, 1]. \tag{4}$$

We call the linear mapping

$$T := B_1 B_0^{-1} : \mathcal{L}_0 \to \mathcal{L}_1, \tag{5}$$

the transition, *while the curve $T(t) = B(t)B_0^{-1}$ is the* transition path.

As mentioned earlier, we are mostly interested in transitions with maximal intermediate symmetry. Notice that, by continuity, $\det B_0$ and $\det B_1$ have the same sign, so that $\det T > 0$. The following equivalent statements characterise lattice transitions.

Proposition 2.3. *Let $\mathcal{L}_0$ and $\mathcal{L}_1$ be two lattices, and $\mathcal{G} \subset \mathcal{P}(\mathcal{L}_0)$. The following statements are equivalent:*

i) There exists a transition between $\mathcal{L}_0$ and $\mathcal{L}_1$ with intermediate symmetry $\mathcal{G}$.

ii) There exist bases B_0 and B_1 of $\mathcal{L}_0$ and $\mathcal{L}_1$, such that for $\tilde{\mathcal{G}} = B_0^{-1}\mathcal{G}B_0$

$$\tilde{\mathcal{G}} \subset \Lambda(B_0) \cap \Lambda(B_1). \tag{6}$$

iii) There exist bases B_0 and B_1 of $\mathcal{L}_0$ and $\mathcal{L}_1$ such that

$$B_1 = RUB_0, \quad with \quad R \in SO(n) \quad and \quad U \in \mathcal{Z}(\mathcal{G}, \mathbb{R}) \cap Sym^+(n, \mathbb{R}). \tag{7}$$

iv) There exist a basis B_0 of $\mathcal{L}_0$, and continuous paths

$$R : [0, 1] \to SO(n), \quad and \quad U : [0, 1] \to \mathcal{Z}(\mathcal{G}, \mathbb{R}) \cap Sym^+(n, \mathbb{R}),$$

such that $R(0) = U(0) = I$ and $R(1)U(1)B_0 = B_1$ is a basis of $\mathcal{L}_1$.

v) There exist bases B_0 and B_1 of $\mathcal{L}_0$ and $\mathcal{L}_1$ and a continuous path $C : [0, 1] \to Sym^+(n, \mathbb{R})$ such that, letting $C_0 = B_0^\top B_0$, $C_1 = B_1^\top B_1$ and $\tilde{\mathcal{G}} = B_0^{-1}\mathcal{G}B_0$, then $C(0) = C_0$, $C(1) = C_1$, and

$$M^\top C(t)M = C(t) \qquad for \ all \quad M \in \tilde{\mathcal{G}} \quad and \quad t \in [0, 1]. \tag{8}$$

Proof. The implications i) $\Rightarrow$ ii) and i) $\Leftrightarrow$ v) are immediate. To prove that ii) $\Rightarrow$ iii), we notice that, by ii), letting $\mathcal{G}_1 = B_1\tilde{\mathcal{G}}B_1^{-1}$, then $B_1^{-1}\mathcal{G}_1B_1 = B_0^{-1}\mathcal{G}B_0$. Hence $\mathcal{G}$ and $\mathcal{G}_1$ are conjugate in $GL(n, \mathbb{R})$: $\mathcal{G} = T^{-1}\mathcal{G}_1T$, with $T = B_1B_0^{-1}$. By the polar decomposition theorem, writing $T = RU$ with $R \in SO(n)$ and $U \in Sym^+(n, \mathbb{R})$, it follows that, for all $G \in \mathcal{G}$ there exists $H \in \mathcal{G}_1$ such that $G = U^{-1}R^{-1}HRU$, i.e., $UG = R^{-1}HRU$. By the uniqueness of the polar decomposition, since G and $R^{-1}HR \in O(n)$, one has

$$G = R^{-1}HR \qquad and \qquad G = U^{-1}GU,$$

and U belongs to the centraliser of $\mathcal{G}$ in $GL(n, \mathbb{R})$. This proves iii). Notice that, as a by-product of the above argument, $\mathcal{G}$ and $\mathcal{G}_1$ are conjugate in $SO(n)$, indeed

$$\mathcal{G} = R^{-1}\mathcal{G}_1R.$$

To prove that iii) $\Rightarrow$ iv), notice first that $SO(n)$ is arcwise connected, so that there exist paths connecting R to the identity. Further, since U is positive definite, we can write $U = Q^\top DQ$, with $Q \in SO(n)$, $D = \mathrm{diag}(\lambda_1, \ldots, \lambda_n)$, and $\lambda_i > 0$. Then a path connecting U to the identity is for instance $U(t) = Q^\top D(t)Q$, with $D(t) = \mathrm{diag}((\lambda_1 - 1)t + 1, \ldots, (\lambda_n - 1)t + 1)$, which is still in the centraliser. In fact, if $U \in \mathcal{Z}(\mathcal{G}, \mathbb{R})$, then $D \in \mathcal{Z}(Q\mathcal{G}Q^\top, \mathbb{R})$, which means that $DH = HD$ for every $H \in Q\mathcal{G}Q^\top$. This is equivalent to $\lambda_i h_{ij} = \lambda_j h_{ij}$ for all $i, j = 1, \ldots, n$, where h_{ij} are the entries of H. On the other hand,

this identity is true if and only if $[(\lambda_i - 1)t + 1)]h_{ij} = [(\lambda_j - 1)t + 1]h_{ij}$ for all $t \in [0, 1]$, which implies that $D(t) \in \mathcal{Z}(Q\mathcal{G}Q^\top, \mathbb{R})$, so that $U(t) \in \mathcal{Z}(\mathcal{G}, \mathbb{R})$ for all $t \in [0, 1]$.

Finally, iv) $\Rightarrow$ i): in fact, letting $B(t) = R(t)U(t)B_0$, one has

$$
\begin{aligned}
B(t)\tilde{\mathcal{G}}B(t)^{-1} &= R(t)U(t)B_0\tilde{\mathcal{G}}B_0^{-1}U^{-1}(t)R^{-1}(t) \\
&= R(t)U(t)\mathcal{G}U^{-1}(t)R^{-1}(t) = R(t)\mathcal{G}(t)R^{-1}(t) \subset O(n), \quad t \in [0, 1].
\end{aligned}
$$

Hence, $\tilde{\mathcal{G}} \subset \Lambda(B(t))$ for every $t \in [0, 1]$ which proves the claim.

If $T(t) = R(t)U(t)$ is a transition path with symmetry $\mathcal{G}$ between the lattices $\mathcal{L}_0$ and $\mathcal{L}_1$, the symmetry of the intermediate phase is also described by the group of orthogonal transformations

$$
\mathcal{G}_t = T(t)\mathcal{G}T^{-1}(t) = R(t)\mathcal{G}R^{-1}(t), \tag{9}
$$

which is a subgroup of the point group $\mathcal{P}(B(t))$ of the intermediate phase.

The following result is an immediate consequence of the above characterisation of lattice transitions, and shows that any centraliser of $\mathcal{G}$, not necessarily symmetric, defines a transition with that symmetry.

Corollary 2.4. *Any continuous path*

$$
T : [0, 1] \to \mathcal{Z}(\mathcal{G}, \mathbb{R}), \qquad T(0) = I, T(1) = B_1B_0^{-1},
$$

with B_0 and B_1 lattice bases for $\mathcal{L}_0$ and $\mathcal{L}_1$, defines a transition between $\mathcal{L}_0$ and $\mathcal{L}_1$ with intermediate symmetry $\mathcal{G}$.

3 Cut-and-project quasicrystals and canonical tilings

Let $\mathcal{L}$ be a n-dimensional lattice with point group $\mathcal{P} = \mathcal{P}(\mathcal{L})$. Consider a subgroup $\mathcal{H}$ of $\mathcal{P}$, and assume that there exists a k-dimensional subspace $E \subset \mathbb{R}^n$ invariant under $\mathcal{H}$. Denote by $E^\perp$ the orthogonal complement of E, so that

$$
\mathbb{R}^n = E \oplus E^\perp,
$$

with $\pi : \mathbb{R}^n \to E$ and $\pi^\perp : \mathbb{R}^n \to E^\perp$ the corresponding projection operators. Also, denote by $\mathcal{U} \subset \mathbb{R}^n$ a fundamental domain of $\mathcal{L}$ acting on $\mathbb{R}^n$ as a translation group, such as, for instance, the Voronoi cell at $\boldsymbol{x}_0 \in \mathcal{L}$ (cf. e.g., Senechal (1996)):

$$
\mathcal{U} = \mathcal{V}(\boldsymbol{x}_0) = \{\boldsymbol{x} \in \mathbb{R}^n : |\boldsymbol{x} - \boldsymbol{y}| \geq |\boldsymbol{x} - \boldsymbol{x}_0|, \ \forall \boldsymbol{y} \in \mathcal{L}\}.
$$

The Voronoi cell at the origin is invariant under the point group of the lattice Senechal (1996), and hence also under $\mathcal{H}$. Notice that the collection of all the Voronoi cells of the n-dimensional lattice defines a cell complex in $\mathbb{R}^n$. We assume that $\mathcal{U} = \mathcal{V}(\boldsymbol{0})$ from now on.

Fix now a regular shift vector in $\mathbb{R}^n$, i.e., a vector $\boldsymbol{\gamma}$ (possibly $\mathbf{0}$) such that

$$(\boldsymbol{\gamma} + E) \cap \mathcal{F} = \emptyset$$

for every d-dimensional facet $\mathcal{F}$ of $\mathcal{V}(\boldsymbol{x}_0)$, with $d < n - k$, and for all $\boldsymbol{x}_0 \in \mathcal{L}$. Defining the projection window as

$$\mathcal{W} = \pi^\perp(\mathcal{U}) \subset E^\perp,$$

a cut-and-project quasicrystal is the point set given by

$$(\mathcal{L}, E) := \{\pi(\boldsymbol{x}) \, : \, \pi^\perp(\boldsymbol{\gamma}) - \pi^\perp(\boldsymbol{x}) \in \mathcal{W}\} \subset E. \tag{10}$$

When E is totally irrational, i.e., $E \cap \mathcal{L}^* = \{\mathbf{0}\}$, with $\mathcal{L}^*$ the dual lattice, the set $\pi(\mathcal{L})$ is dense in E; otherwise it is a $\mathbb{Z}$-module, possibly a lattice, in E. We refer to the point set $(\mathcal{L}, E)$ as *quasicrystal*.

There exists a canonical method for constructing aperiodic tilings of the space E using the points of a cut-and-project quasicrystal as vertices (Katz, 1989; Kramer and Schlottmann, 1989). Indeed, the complex of the Voronoi cells of the n-dimensional lattice defines a periodic tiling of $\mathbb{R}^n$; its dual complex is also a periodic tiling of $\mathbb{R}^n$, called the Delone tiling, constructed as follows: if $\mathcal{F}$ is a p-facet of a Voronoi cell, i.e., a p-cell of the Voronoi complex, its dual cell $\mathcal{F}^*$ has dimension $n - p$ and is the convex hull of the centers of the Voronoi cells that intersect in $\mathcal{F}$, i.e., letting

$$M^*(\mathcal{F}) = \{\boldsymbol{x} \in \mathcal{L} \, : \, \mathcal{F} \subseteq \mathcal{V}(\boldsymbol{x})\},$$

then

$$\mathcal{F}^* = \text{conv}(M^*(\mathcal{F})),$$

where $\text{conv}(M^*(\mathcal{F}))$ is the convex hull of the lattice points in $M^*(\mathcal{F})$.

The Delone tiling of $\mathbb{R}^n$ induces a tiling of E by projection on E of those Delone k-facets dual to the $(n - k)$-facets of the Voronoi tiling that have non-empty intersection with $\boldsymbol{\gamma} + E$, where $k = \dim E$. By construction, the tiling of E thus obtained has vertices at the points of the corresponding quasicrystal. If $\boldsymbol{\gamma}$ is invariant under $\mathcal{H}$, and if we choose $\mathcal{W}$ to be the projection on $E^\perp$ of the Voronoi cell at the origin $\mathcal{V}(\mathbf{0})$, the associated tiling is invariant under the representation of $\mathcal{H}$ in E. In fact, $\mathcal{H}$ commutes with the projection π, so that $\mathcal{H}$-orbits in $\mathbb{R}^n$ project on $\mathcal{H}^\|$-orbits in E, with $\mathcal{H}^\|$ the representation of $\mathcal{H}$ in E.

For $\boldsymbol{y} = \pi(\boldsymbol{x})$ a point of a cut-and-project quasicrystal, the vertex star at $\boldsymbol{y}$ is the set of all tiles of E that have $\boldsymbol{y}$ as one of their vertices. It can be shown (Senechal, 1996) that all the vertex stars of a tiling obtained by dualisation are determined by the intersections of the projections on $E^\perp$ of the $(n - k)$-dimensional facets of the Voronoi cell $\mathcal{V}(\mathbf{0})$. In fact, $\boldsymbol{y} = \pi(\boldsymbol{x})$ is the vertex of a tile $\pi(\mathcal{F}^*)$ if $\pi^\perp(\boldsymbol{\gamma}) - \pi^\perp(\boldsymbol{x}) \in \pi^\perp(\mathcal{F})$, where $\mathcal{F}$ is a $(n - k)$-dimensional facet of the Voronoi cell $\mathcal{V}(\mathbf{0})$. Hence, for instance, the number

of tiles of which $\boldsymbol{y}$ is a vertex is just the number of projected facets to which $\pi^{\perp}(\boldsymbol{\gamma}) - \pi^{\perp}(\boldsymbol{x})$ belongs.

When $\boldsymbol{\gamma}$ is not regular, and a lattice point $\boldsymbol{x} \in \mathcal{L}$ is such that $\pi^{\perp}(\boldsymbol{\gamma}) - \pi^{\perp}(\boldsymbol{x})$ belongs to the common boundary $\mathcal{B}$ of the projection of two, or more, $(n-k)$-dimensional facets of the Voronoi cell, then $\pi(\boldsymbol{x})$ is a vertex of all tiles dual to Voronoi facets intersecting in $\mathcal{B}$, and these tiles may overlap. In this case, to avoid self-intersections, we use as tile the projection on E of the dual of the low-dimensional facet $\mathcal{B}$: these are called glue tiles (Kramer, 2002).

The techniques summarised above have been extensively applied in the study of quasicrystals and tilings of the plane and space (de Bruijn, 1981; Katz, 1989; Reiter, 2002; Kramer and Neri, 1984; Rokhsar and Mermin, 1987; Janot, 1989; Papadopolos et al., 1997, 1998, 1993).

4   Structural transformations of cut-and-project quasicrystals

We now indicate how structural transformations of cut-and-project quasicrystals can be induced by transitions between higher-dimensional lattices. Consider two n-dimensional lattices $\mathcal{L}_0$ and $\mathcal{L}_1$, with point groups $\mathcal{P}(\mathcal{L}_0)$ and $\mathcal{P}(\mathcal{L}_1)$, and two subgroups $\mathcal{H}_0 \subset \mathcal{P}(\mathcal{L}_0)$ and $\mathcal{H}_1 \subset \mathcal{P}(\mathcal{L}_1)$. Assume that $\mathcal{H}_0$ and $\mathcal{H}_1$ have invariant subspaces E_0 and E_1, respectively, with $\dim E_0 = \dim E_1 = k$. Without loss of generality, assume that

$$E_0 = E_1 =: E,$$

and consider the cut-and-project quasicrystals $(\mathcal{L}_0, E)$ and $(\mathcal{L}_1, E)$.

Definition 4.1. *We say that there exists a transition between the cut-and-project quasicrystals $(\mathcal{L}_0, E)$ and $(\mathcal{L}_1, E)$ with intermediate symmetry $\mathcal{G} \subset \mathcal{P}(\mathcal{L}_0)$ if there exists a transition with intermediate symmetry $\mathcal{G}$ between $\mathcal{L}_0$ and $\mathcal{L}_1$ such that for $T(t) = R(t)U(t)$, with $R(t) \in SO(n)$ and $U(t) \in Sym^+(n, \mathbb{R}) \cap \mathcal{Z}(\mathcal{G}, \mathbb{R})$, E is invariant under $\mathcal{G}_t$, i.e.,*

$$\mathcal{G}_t E \subset E, \qquad t \in [0, 1], \tag{11}$$

with

$$\mathcal{G}_t = R(t)^{\top} \mathcal{G} R(t) \subset \mathcal{P}(\mathcal{L}_t), \qquad \mathcal{L}_t = T(t)\mathcal{L}_0. \tag{12}$$

Any such transition defines a family of cut-and-project quasicrystals $(\mathcal{L}_t, E)$ in the same projection space E, all of which have symmetry $\mathcal{G}$.

It is useful to discuss the relation of our method with other higher-dimensional approaches used in the literature to study experimentally observed transitions between icosahedral quasicrystals and cubic phases in 3D (Kramer, 1987; Litvin et al., 1987; Li et al., 1989a,b; Li and Cheng, 1990;

Torres et al., 1989; Aragón and Torres, 1991; Mukhopadhya et al., 1991; Cheng et al., 1992; Sun, 1993), and for deformations of Penrose tilings of the plane (cf., for instance, Ishii (1993), Sing and Welberry (2006), Welberry and Sing (2007)). As mentioned in Sect. 6, icosahedral quasicrystals can be obtained by projection of a simple cubic lattice in 6D on a 3D subspace that carries an irreducible representation of the icosahedral group. The procedure used to obtain a transformation of the projected 3D point set in these works is either (i) by rotating the projection plane with respect to the 6D lattice or (ii) by deforming the 6D lattice through certain linear transformations called phason strains. These two approaches can be shown to be related (Cheng et al., 1992). The technique presented in this paper generalises (i) and (ii), since it allows for both deformations and changes of symmetry of the lattice, controlling the intermediate symmetry. In detail our approach relates to the rotation-plane method (Kramer, 1987) as follows. For a fixed 6D cubic lattice $\mathcal{L}$, it is known that suitable choices of 3D subspaces E_0 and E_1 in $\mathbb{R}^6$ yield sets $(\mathcal{L}, E_0)$ and $(\mathcal{L}, E_1)$ that correspond to a FCC crystal or to an icosahedral quasicrystal in $\mathbb{R}^3$. Suppose that $\mathcal{H}_0$ and $\mathcal{H}_1$ are 6D representations of the 3D cubic group O and of the icosahedral group, respectively, so that E_0 is invariant under $\mathcal{H}_0$ and E_1 is invariant under $\mathcal{H}_1$. Then there exist orthonormal bases $\tilde{B}_0$ and $\tilde{B}_1$ of $\mathbb{R}^6$ (not necessarily lattice bases) that block-diagonalise $\mathcal{H}_0$ and $\mathcal{H}_1$ as the direct sum of two 3D blocks. These bases are adapted to the subspaces E_0 and E_1.

Consider now the tetrahedral group $\mathcal{T}$, which is a subgroup of both $\mathcal{H}_0$ and $\mathcal{H}_1$: both $\tilde{B}_0$ and $\tilde{B}_1$ block-diagonalise $\mathcal{T}$, but since $\mathcal{T}$ has just a single 3D irreducible representation, we may choose $\tilde{B}_0$ and $\tilde{B}_1$ such that $\tilde{B}_1^{-1} \mathcal{T} \tilde{B}_1 = \tilde{B}_0^{-1} \mathcal{T} \tilde{B}_0 = \mathcal{T}'$. Hence, there exists $C \in SO(6)$ in the centraliser of $\mathcal{T}'$ such that $\tilde{B}_1 = \tilde{B}_0 C$. Actually, there exists a continuous path $C(t)$ in the centraliser of $\mathcal{T}'$ that connects C to the identity (the 'Schur rotation'). This in turn means that the path $R(t) = \tilde{B}_0 C(t) \tilde{B}_0^{-1}$ belongs to the centraliser of $\mathcal{T}$ in $SO(6)$, and is such that $\tilde{B}_1 = R(1)\tilde{B}_0$. To summarise, the Schur rotation defines a path in the centraliser of $\mathcal{T}$, connecting E_0 to E_1, i.e., such that $E_1 = R(1)E_0$, and $R(t)E_0$ is invariant under $\mathcal{T}$ for every $t \in [0, 1]$.

The Schur rotation can be used to define a transition with intermediate symmetry $\mathcal{T}$ in the sense of the present paper because rotating the projection plane with respect to the lattice is equivalent to rotating the lattice with respect to a fixed projection plane: in fact, E_0 is invariant under both $R(1)^{\top} \mathcal{H}_1 R(1)$ and $R(t)^{\top} \mathcal{T} R(t)$, and since $\mathcal{P}(R(1)^{\top} \mathcal{L}_0) = R(1)^{\top} \mathcal{P}(\mathcal{L}_0) R(1)$, this means that the Schur rotation defines a family of rotated cubic 6D lattices

$$\mathcal{L}_t := R^{\top}(t)\mathcal{L}, \quad \mathcal{L}_1 := R^{\top}(1)\mathcal{L},$$

with the property that $R(t)^{\top} \mathcal{T} R(t)$-orbits in $\mathcal{L}_t$ project on tetrahedral orbits

11

in E_0. Consider now any path

$$U : [0,1] \to Sym^+(n,\mathbb{R}) \cap \mathcal{Z}(\mathcal{T},\mathbb{R}), \qquad U(0) = U(1) = I.$$

Then, choosing any lattice basis B_0 for $\mathcal{L}_0$, the path

$$B(t) = R(t)U(t)B_0, \qquad t \in [0,1],$$

defines a lattice transition with tetrahedral symmetry between $\mathcal{L}$ and $\mathcal{L}_1$. Furthermore, since $\mathcal{T}_t = R(t)^\top \mathcal{T} R(t)$ and $R(1)^\top \mathcal{H}_1 R(1)$ have E_0 as invariant subspace, this transition defines in turn a transition between the quasicrystals $(\mathcal{L}, E_0)$ and $(\mathcal{L}_1, E_0)$ with tetrahedral symmetry (cf. (11) and (12)).

5 Transformations between planar aperiodic tilings preserving the five-fold symmetry

In this section we present three examples of transformations that preserve the global five-fold symmetry between planar tilings having that same symmetry, in particular the Penrose tiling. For the latter, we adopt here a 5-dimensional approach instead of the usual one based on a 4D minimal embedding (Baake et al., 1990b), because in this way it is simpler to describe the transitions in terms of deformations of the unit cubic cell in $\mathbb{R}^5$.

Consider the SC, BCC, and FCC lattices, and the standard basis (e_α), $\alpha = 1, \ldots, 5$, in $\mathbb{R}^5$, together with the group $\mathcal{G} = C_5 \subset SO(5)$ of five-fold rotations about the body diagonal $\boldsymbol{n}$ of the unit cube:

$$\boldsymbol{n} = \sum_{\alpha=1}^{5} \boldsymbol{e}_\alpha.$$

The group $\mathcal{G}$, which leaves all the three above 5D cubic lattices invariant, has two mutually orthogonal invariant subspaces: the 2D subspace E and the 3D subspace $E^\perp$ with projections

$$\pi = \begin{pmatrix} 1 & \cos(2\pi/5) & \cos(4\pi/5) & \cos(6\pi/5) & \cos(8\pi/5) \\ 0 & \sin(2\pi/5) & \sin(4\pi/5) & \sin(6\pi/5) & \sin(8\pi/5) \end{pmatrix}$$

and

$$\pi^\perp = \begin{pmatrix} 1 & \cos(4\pi/5) & \cos(8\pi/5) & \cos(2\pi/5) & \cos(6\pi/5) \\ 0 & \sin(4\pi/5) & \sin(8\pi/5) & \sin(2\pi/5) & \sin(6\pi/5)6c \\ 1 & 1 & 1 & 1 & 1 \end{pmatrix}.$$

Notice that $E^\perp$ may in turn be split as the direct sum of two orthogonal invariant subspaces, a 2D plane and a line parallel to $\boldsymbol{n}$.

With reference to Sect. 3, we choose $\boldsymbol{\gamma} = \frac{1}{2}\boldsymbol{n}$; projection of the SC lattice $(3)_1$ and the related Delone tiling on E produces the well-known Penrose

tiling of the plane, while projecting the FCC and BCC lattices in $(3)_{2,3}$ gives more complex aperiodic planar tilings (Fig. 7), see also Reiter (2002). All these aperiodic structures have a global five-fold symmetry about the origin, and our focus are their structural transformations preserving such symmetry.

Proposition 2.3 guarantees that the C_5-preserving transition paths for the associated 5D lattices are parametrised by the centralisers of C_5 in $GL(5, \mathbb{R})$, i.e., the group of matrices which has explicitly the form, for $x, y, z, s, v \in \mathbb{R}$:

$$
M = \begin{pmatrix}
x & y & z & s & v \\
v & x & y & z & s \\
s & v & x & y & z \\
z & s & v & x & y \\
y & z & s & v & x
\end{pmatrix}.
$$

We consider three specific transition paths: the first two are paths between the SC and the BCC lattices in 5D:

$$
T_1(t) = \begin{pmatrix}
1 - t/2 & t/2 & t/2 & -t/2 & -t/2 \\
-t/2 & 1 - t/2 & t/2 & t/2 & -t/2 \\
-t/2 & -t/2 & 1 - t/2 & t/2 & t/2 \\
t/2 & -t/2 & -t/2 & 1 - t/2 & t/2 \\
t/2 & t/2 & -t/2 & -t/2 & 1 - t/2
\end{pmatrix}, \quad (13)
$$

and

$$
T_2(t) = \begin{pmatrix}
1 - t/2 & t/2 & -t/2 & t/2 & -t/2 \\
-t/2 & 1 - t/2 & t/2 & -t/2 & t/2 \\
t/2 & -t/2 & 1 - t/2 & t/2 & -t/2 \\
-t/2 & t/2 & -t/2 & 1 - t/2 & t/2 \\
t/2 & -t/2 & t/2 & -t/2 & 1 - t/2
\end{pmatrix}, \quad (14)
$$

while the third one joins the SC to the FCC lattice:

$$
T_3(t) = \begin{pmatrix}
1 - t/2 & 0 & 0 & 0 & t/2 \\
t/2 & 1 - t/2 & 0 & 0 & 0 \\
0 & t/2 & 1 - t/2 & 0 & 0 \\
0 & 0 & t/2 & 1 - t/2 & 0 \\
0 & 0 & 0 & t/2 & 1 - t/2
\end{pmatrix}. \quad (15)
$$

Each intermediate lattice along these paths has global five-fold symmetry by construction. Since

$$
T_1(t)\boldsymbol{n} = (1 - t/2)\boldsymbol{n}, \qquad T_2(t)\boldsymbol{n} = (1 - t/2)\boldsymbol{n},
$$

the first two transition paths above involve a compression of the unit cube along a body diagonal $\boldsymbol{n}$. These paths entail, through the dualisation technique applied at each step, also transformations between the Penrose and

13

the BCC and FCC tilings. For a point $\boldsymbol{x} \in \mathcal{L}$ of a high-dimensional lattice, the tiles which have $\pi(\boldsymbol{x})$ as a vertex are the projections on E of the 2D duals of the 3D facets $\mathcal{F}$ of $\mathcal{V}(\boldsymbol{0})$ such that $\pi^{\perp}(\boldsymbol{\gamma} - \boldsymbol{x}) \in \pi^{\perp}(\mathcal{F})$. To explain transformations in tilings in E, it is useful to look at the changes in how $\boldsymbol{\gamma} - \boldsymbol{x}$ is projected into these projected facets. As a general observation, we see that the transformations of the aperiodic structures proceed through a combination of three basic mechanisms:

(1) *Splitting of a tile into two:* This occurs when a facet of the Voronoi cell splits into two. The projection on $E^{\perp}$ of the facet before the split, and the two new facets, are shown in Fig. 3(a). A lattice point $\boldsymbol{x}$ such that $\pi^{\perp}(\boldsymbol{\gamma} - \boldsymbol{x})$ belongs to the region where the perpendicular projections overlap will be a vertex of a single tile in the first step and two tiles in the subsequent step (Fig. 3(b)). Equivalently, two tiles join to become a single tile if the projection of $\boldsymbol{\gamma} - \boldsymbol{x}$ falls out of the intersection of two regions into a region covered by only one.
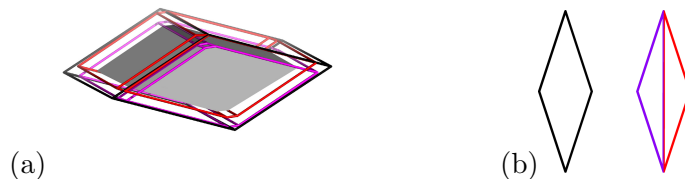

(a) (b)

Figure 3: (a) The splitting of a Voronoi facet into two: the larger rhombo-hedron is the projection on $E^{\perp}$ of the facet before splitting, the two smaller overlapping regions with shaded intersection being the projection of the split facet. (b) The rhomb on the left corresponds to the projection on E of the dual of the facet before splitting, while the two triangular tiles correspond to the duals of the two split facets.

(2) *Tile flips:* Rearrangements of tiles within limited areas, which we call tile flips, occur due to points $\pi^{\perp}(\boldsymbol{\gamma} - \boldsymbol{x})$ in $E^{\perp}$ moving from one pro-jected facet in $E^{\perp}$ to another, such as going through the shaded area in Fig. 4(a). In the upper half of the figure, the point $\boldsymbol{\gamma} - \boldsymbol{x}$ is projected into the projection of two Voronoi regions in $E^{\perp}$, and therefore $\pi(\boldsymbol{x})$ is a vertex of two tiles as shown on the left of Fig. 4(b). When the projected point goes through the shaded face, it is now only within the projection of a single Voronoi facet and $\pi(\boldsymbol{x})$ is thus a vertex of a single tile. Since the transitions are continuous, there is a time when a projected lattice point lies in the intersection of these regions pro-ducing overlapping tiles, and at this time we insert in the tiling a glue tile, in this case a quadrilateral tile.
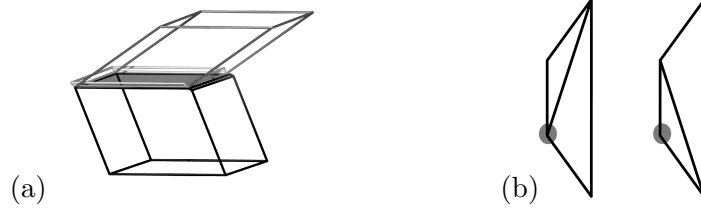
14

Figure 4: (a) The projection on $E^\perp$ of three 3D facets of $\mathcal{V}(\mathbf{0})$ for some lattice $\mathcal{L}$, two above the shaded face and one below. (b) Along a transition path a projected lattice point, corresponding to the shaded vertex in the tiles in E, passes from the two regions at the top of the shaded face to the lower region when projected on $E^\perp$. This results in a tile flip.

(3) *Tile mergers:* During the lattice transition the Voronoi cells change, so that the projection on $E^\perp$ may involve different sets of points, see for instance Fig. 5(a). Points $\boldsymbol{x}$ such that $\pi^\perp(\boldsymbol{\gamma} - \boldsymbol{x})$ fall outside the resulting acceptance window are deleted from the tiling, along with any tiles with these points as vertices. This produces tile mergers as seen for instance in Fig. 5(b).

Figure 5: (a) The projections on $E^\perp$ of the Voronoi cells on the path (15), at $t = 0$ (lines) and $t = 0.3$ (shaded area). (b) The central vertex is the image of a lattice point projected near the boundary of the shrinking Voronoi cell. As the Voronoi cell shrinks, the point is no longer in the acceptance window, and is hence removed from the tiling.

All the changes in the transforming quasicrystals and tilings can be described through the three mechanisms above. Fig. 7 shows four steps in the transformations from SC to BCC along the paths defined by (13) and (14), as well as the transformation from SC to FCC defined by the path in (15). Fig. 7(a) shows the tiling for $t = 0$, obtained via projection from a simple cubic lattice, which then branches into three pathways. For the path (13) shown in Fig. 7(b),(c) and (f), the first step in the transition is a splitting of all tiles along their long diagonal, followed by flips, deletions of vertices and further splits/recombinations. The second path (14) shown

15

in Fig. 7(d),(e) and (f) also displays at first a splitting of all the tiles, in this case along the shorter diagonal, and then proceeds as above to further splits/recombinations. For the transition from SC to FCC (15), Fig. 7(g),(h) and (i), only the thin rhombs split at first, followed by further changes in the tiles, finally resulting in a much coarser tiling than the one produced by the BCC lattice.

6   Example of a transformation between icosahedral 3D quasicrystals

We briefly discuss here a transformation between icosahedral quasicrystals in $\mathbb{R}^3$ and their associated tilings. Related ideas are analysed in more detail in Indelicato et al. (2011), where a technique similar the present one has been applied to study the configurational changes of icosahedral viral capsids.

The two- and three-fold rotations

$$
G_2 = \begin{pmatrix} -1 & 0 & 0 & 0 & 0 & 0 \\ 0 & -1 & 0 & 0 & 0 & 0 \\ 0 & 0 & 0 & 0 & 1 & 0 \\ 0 & 0 & 0 & 0 & 0 & 1 \\ 0 & 0 & 1 & 0 & 0 & 0 \\ 0 & 0 & 0 & 1 & 0 & 0 \end{pmatrix}, \quad
G_3 = \begin{pmatrix} 0 & -1 & 0 & 0 & 0 & 0 \\ 0 & 0 & -1 & 0 & 0 & 0 \\ 1 & 0 & 0 & 0 & 0 & 0 \\ 0 & 0 & 0 & 0 & 0 & 1 \\ 0 & 0 & 0 & 1 & 0 & 0 \\ 0 & 0 & 0 & 0 & 1 & 0 \end{pmatrix},
$$
(16)

generate a 6D integral representation of the icosahedral group $\mathcal{I}$ (cf. e.g., Katz (1989)). The matrix group $\mathcal{I}$ leaves the three 6D cubic lattices (SC, FCC, BCC, cf. (3)) invariant and is a subgroup of the hyperoctahedral group B_6 (Levitov and Rhyner, 1988).

The representation of $\mathcal{I}$ on $\mathbb{R}^6$ is the sum of two non-equivalent irreducible representations of degree 3 (Katz, 1989), and $\mathbb{R}^6$ splits into the direct sum of two 3D subspaces, E and $E^\perp$, invariant under the icosahedral group. In particular, following Katz (1989), we choose as matrix representation of the projection on E

$$
\pi = \begin{pmatrix} \tau & 0 & -1 & 0 & \tau & 1 \\ 1 & \tau & 0 & -\tau & -1 & 0 \\ 0 & 1 & \tau & 1 & 0 & \tau \end{pmatrix}
$$

with $\tau = \frac{1}{2}(1 + \sqrt{5})$. Notice that the vectors of the 6D canonical basis project on vectors pointing to the vertices of an icosahedron.

The icosahedral group $\mathcal{I}$ has three maximal subgroups: the tetrahedral group $\mathcal{T}$ and the dihedral groups D_5 and D_3. We are interested in transitions between the SC and the FCC, BCC lattices with maximal intermediate symmetry, described by one of these subgroups. However, there exist no tetrahedral transition paths among the cubic lattices in 6D. We show this for

transitions between the SC and FCC lattices, a similar proof being possible also for transitions to a BCC lattice. Indeed, assume that a tetrahedral transition exists. Then, according to Prop. 2.3-(iii) the transition operators T can be decomposed as $T = RU$, with $R \in SO(n)$ and $U \in \mathcal{Z}(\mathcal{T}, \mathbb{R}) \cap Sym^+(n, \mathbb{R})$ such that

$$B_1 = RUB_0,$$

with B_0 a basis of a SC lattice and B_1 a basis of an FCC lattice. Any $U \in \mathcal{Z}(\mathcal{T}, \mathbb{R}) \cap Sym^+(n, \mathbb{R})$ has the form (Indelicato et al., 2011):

$$U = \begin{pmatrix} z & -x & -y & x & -x & -x \\ -x & z & -x & x & x & y \\ -y & -x & z & -x & x & -x \\ x & x & -x & z & y & -x \\ -x & x & x & y & z & -x \\ -x & y & -x & -x & -x & z \end{pmatrix},$$

with $x, y, z \in \mathbb{R}$. By 3 the metric of an FCC lattice $C = B_1^\top B_1$ has entries in $\mathbb{Z}/4$, and since

$$C = B_1^\top B_1 = B_0^\top U^\top R^\top R U B_0 = B_0^\top U^2 B_0$$

and $B_0 \in GL(n, \mathbb{Z})$, also $U^2 = B_0^{-\top} C B_0^{-1}$ has entries in $\mathbb{Z}/4$:

$$U^2 = \begin{pmatrix} a & -b & -c & b & -b & -b \\ -b & a & -b & b & b & c \\ -c & -b & a & -b & b & -b \\ b & b & -b & a & c & -b \\ -b & b & b & c & a & -b \\ -b & c & -b & -b & -b, & a \end{pmatrix},$$

with $a = z^2 + 4x^2 + y^2$, $b = 2xz$, $c = 2yz$, and $a, b, c \in \mathbb{Z}/4$.

Then $det(U^2) = det(B_0^{-\top} C B_0^{-1})$ leads to the following equation

$$[a^2 - 4b^2 - c^2]^3 = \left(\frac{1}{2}\right)^{10}$$

that can not be fulfilled for any choice of $a, b, c \in \mathbb{Z}/4$. Infact, for $a = \alpha/4$, $b = \beta/4$, $c = \gamma/4$ with $\alpha, \beta, \gamma \in \mathbb{Z}$ the equation above reduces to

$$\left(\alpha^2 - 4\beta^2 + \gamma^2\right)^3 = 4,$$

which cannot be solved by any integer α, β, γ. A similar argument shows that there cannot be tetrahedral transitions between the SC and any rescaled FCC and BCC lattices. The same holds also for the FCC-BCC lattice transitions in 6D.

We consider next the possibility of transitions with D_5 symmetry (see more details in Indelicato et al. (2011)). As discussed above, such transitions belong to the centraliser of D_5, having the form:

$$T = T(x, y, z, s, u, w) = \begin{pmatrix} z & x & y & y & x & s \\ x & z & x & y & y & s \\ y & x & z & x & y & s \\ y & y & x & z & x & s \\ x & y & y & x & z & s \\ v & v & v & v & v & w \end{pmatrix}, \tag{17}$$

where x, y, z, s, u, w depend on t. As an example, we consider a path with intermediate symmetry D_5 that deforms an SC lattice (at $t = 0$) into an FCC lattice (at $t = 1$):

$$T(t) = \begin{pmatrix} 1 - \frac{1}{2}t & 0 & 0 & 0 & 0 & 0 \\ 0 & 1 - \frac{1}{2}t & 0 & 0 & 0 & 0 \\ 0 & 0 & 1 - \frac{1}{2}t & 0 & 0 & 0 \\ 0 & 0 & 0 & 1 - \frac{1}{2}t & 0 & 0 \\ 0 & 0 & 0 & 0 & 1 - \frac{1}{2}t & 0 \\ \frac{1}{2}t & \frac{1}{2}t & \frac{1}{2}t & \frac{1}{2}t & \frac{1}{2}t & 1 \end{pmatrix}. \tag{18}$$

Fig. 6 shows three snapshots of a patch of the corresponding 3D tiling around a fixed vertex, i.e., projections on E of a suitable portion of the Delone tiling of the lattices $\mathcal{L}(B(t))$, for $t = 0; 0.233;$ and 1. Throughout the transition the tile arrangements have D_5 symmetry, and we observe they evolve through mechanisms similar to those discussed in detail for the planar case in Sect. 5.

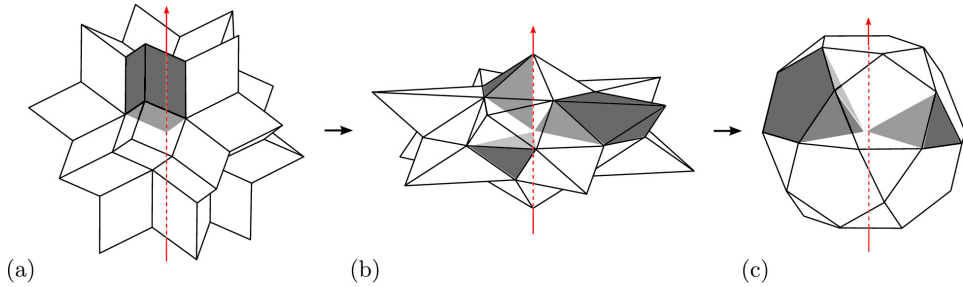(a)   (b)   (c)

Figure 6: Vertex stars at the origin of the tilings obtained by projection of (a) the 6D SC lattice, (b) an intermediate D_5 lattice and (c) the FCC lattice. The vertex star is composed by repetitions of a number of suitable tiles, highlighted in the figure. The pentagonal pyramid in (c) is a glue tile.

7 Conclusions

In this work we have proposed a new approach for the investigation of structural transformations in cut-and-project quasicrystals, based on higher dimensional analogs of the classical 3D Bain strains, i.e. deformation paths which maintain a given symmetry, possibly maximal, for the associated higher dimensional lattices during the transition. Our method is related to the phason-strain and rotation-plane techniques (see Sect. 4), but has the advantage of allowing for more general transitions between the higher dimensional lattices, possibly involving also different Bravais types, and takes explicitly into account all possible intermediate symmetries.

The main purpose of our work is to explore the effect these structural transformations have on the plane or space tilings associated with each quasicrystal, for instance by means of the dualisation method. The local tile rearrangements can be understood in terms of the change of geometry of the Voronoi cell of the higher dimensional lattice during the transition, and we analyse the effect this has on the projected lattice points. Our results suggest that the possible ways in which an aperiodic tiling can change, while still conserving some intermediate symmetry, reduces to the three basic mechanisms of tile splitting, tile flipping, and tile merger.

As case studies, we have examined how the Penrose tiling of the plane changes as the underlying 5D cubic lattice undergoes a deformation to either a BCC or an FCC lattice through a transition path that preserves five-fold symmetry. We have also examined the transformation of an icosahedral Ammann tiling in 3D space, obtained by projecting a suitable deformation path connecting a SC and an FCC lattice in 6D.

A rich landscape for structural transformations in quasicrystals emerges from our approach. The general patterns identified here may provide a basis for further analysis of structural transitions in quasilattices and for a possible classification of transitions in aperiodic structures. This is of interest both from a theoretical viewpoint and for the applications, for instance in virology for the study of the structural rearrangements of viral capsids important for infection.

References

J.L. Aragón and M. Torres. A geometrical approach to icosahedral displacive phase transitions. *Europhys. Lett.*, 15:203–208, 1991.

M. Baake, D. Joseph, P. Kramer, and M. Schlottmann. Root lattices and quasicrystals. *J. Phys. A: Math. Gen.*, 23:L1037 – L1041, 1990a.

M. Baake, P. Kramer, M. Schlottmann, and D. Zeidler. Planar patterns with fivefold symmetry as sections of periodic structures in 4-space. *Int. J. Mod. Phys.*, B4:2217–2268, 1990b.

E. C. Bain. The nature of martensite. *Trans. AIME*, 70:23–35, 1924.

K. Bhattacharya, S. Conti, G. Zanzotto, and J. Zimmer. Crystal symmetry and the reversibility of martensitic transformations. *Nature*, 428:55–59, 2004.

L. L. Boyer. Magic strains in face-centered and body-centered cubic lattices. *Acta Cryst.*, A45:fc29–fc32, 1989.

C. Capillas, J. M. Perez-Mato, and M. I. Aroyo. Maximal symmetry transition paths for reconstructive phase transitions. *J. Phys.: Condens. Matter*, 19:275203, 2007.

Y.F. Cheng, G.Z. Pan, and F.H. Li. Real space approach to the linear phason strain. *Phys. Stat. Sol. (b)*, 170:47–55, 1992.

J. W. Christian. *The theory of transformations in metals and alloys.* Pergamon Press, 2002.

N. G. de Bruijn. Algebraic theory of Penrose's non-periodic tilings of the plane I,II. *Nederl. Akad. Wetensch. Indag. Math.*, 43(1):39–52, 53–66, 1981.

G. Indelicato, P. Cermelli, D. G. Salthouse, S. Racca, G. Zanzotto, and R. Twarock. A crystallographic approach to structural transitions in icosahedral viruses. *J. Math. Biol.*, pages doi:10.1007/s00285–011–0425–5, 2011.

Y. Ishii. Structural transformation and phason dynamics in quasicrystals. *J. Non-Cryst. Solids*, 153-154:645–649, 1993.

C. Janot. The crystallography of quasicrystals. *Proc. R. Soc. Lond. A*, 442 (1914):113–127, 1989.

A. Katz. *Introduction to the Mathematics of Quasicrystals*, chapter Some local properties of the 3-dimensional Penrose tilings, pages 147–182. Academic Press, 1989.

T. Keef and R. Twarock. Affine extensions of the icosahedral group with applications to the three-dimensional organisation of simple viruses. *J. Math. Biol*, 59(3):287–313, 2009.

P. Kramer. Continuous rotation from cubic to icosahedral order. *Acta Cryst.*, A43:486–489, 1987.

P. Kramer. *Covering of Discrete Quasiperiodic Sets*, chapter Voronoi and Delone Clusters in Dual Quasiperiodic Tilings, pages 97–165. Springer-Verlag Berlin Heidelberg, 2002.

P. Kramer and R. Neri. On periodic and non-periodic space fillings of E^m obtained by projection. *Acta Cryst.*, A40:580–587, 1984.

P. Kramer and M. Schlottmann. Dualisation of Voronoi domains and Klotz construction: a general method for the generation of proper space fillings. *J. Phys. A: Math. Gen.*, 22:L1097–L1102, 1989.

L.S. Levitov and J. Rhyner. Crystallography of quasicrystals; application to icosahedral symmetry. *J. Phys. France*, 49(11):1835–1849, 1988.

F.H. Li and Y.F. Cheng. A simple approach to quasicrystal structure and phason defect formulation. *Acta Cryst.*, A46:142–149, 1990.

F.H. Li, G.Z. Pan, and Y.F. Cheng. Transformation from icosahedral phase to body center cubic phase in cut description. *Chinese Phys. Lett.*, 6: 465–468, 1989a.

F.H. Li, G.Z. Pan, S.Z. Tao, M.J. Hui, Z.H. Mai, X.S. Chen, and L.Y. Cai. From quasicrystals to ordinary crystals. *Phil. Mag. B*, 59(5):535–542, 1989b.

D.B. Litvin, V. Kopsky, and J.L. Birman. Symmetry and phase transitions in decagonal quasicrystals. *J. Phys A: Math. Gen.*, 20:6169–6184, 1987.

A. L. Mackay. Crystallography and the Penrose pattern. *Physica A*, 114: 609–613, 1982.

N.K. Mukhopadhya, N. Ishihara, S. Ranganathan, and K. Chattopadhyay. Rational approximant structures and phason strain in icosahedral quasicrystalline phases. *Acta metall. mater*, 39(6):1151–1159, 1991.

K. Niizeki. Bravais quasilattices of icosahedral quasicrystals. *Phys. Rev. Letters*, 93(4):045501, 2004.

Z. Papadopolos, P. Kramer, and D. Zieidler. The F-type icosahedral phase - tilings and vertex models. *J. Non-cryst. solids*, 153-154:215–220, 1993.

Z. Papadopolos, R. Klitzing, and P. Kramer. Quasiperiodic icosahedral tilings from the six-dimensional bcc lattice. *J. Phys. A: Math. Gen.*, 30: L143–L147, 1997.

Z. Papadopolos, P. Kramer, and W. Liebermeister. Atomic positions for the icosahedral F-phase tiling. In S. Takeuchi and T. Fujiwara, editors, *Proc. 6th Int. Conf. Quasicrystals 1997*, pages 71–76. World Scientific, Singapore, 1998.

J. Patera and R. Twarock. Affine extensions of noncrystallographic Coxeter groups and quasicrystals. *Journal of Physics A: Mathematical and General*, 35:1551–1574, 2002.

R. Penrose. Pentaplexity. *Eureka*, 39:16–22, 1978.

M. Pitteri and G. Zanzotto. *Continuum models for phase transitions and twinning in crystals*. CRC/Chapman and Hall, London, 2002.

C. A. Reiter. Atlas of quasicrystalline tilings. *Chaos Solitons Fract.*, 14(7): 937–963, 2002.

D. S. Rokhsar and N.D. Mermin. Rudimentary quasicrystallography: the icosahedral and decagonal reciprocal lattices. *Phys. Rev. B*, 35(11):5487–5495, 1987.

M. Senechal. *Quasicrystals and Geometry*. Cambridge University Press, 1996.

D. Shechtman, I. Blech, D. Gratias, and J.W. Cahn. Metallic phase with long-range order and no translational symmetry. *Phys. Rev. Lett.*, 53: 1951–1953, 1984.

B. Sing and T. R. Welberry. Deformed model sets and distorted Penrose tilings. *Z. Krystallogr.*, 221:621–634, 2006.

J. Sun. Structure transitions of the three-dimensional Penrose tiling under phason strain field. *Chinese Phys. Lett.*, 10:449–452, 1993.

P. Toledano and V. Dmitriev. *Reconstructive Phase Transitions: in crystals and quasicrystals*. World Scientific Publishing Company, 1996.

M. Torres, G. Pastor, I. Jimenez, and J. Fayos. Geometric models for continuous transitions from quasicrystals to crystals. *Phil. Mag. Letters*, 59: 181–188, 1989.

A. P. Tsai. Icosahedral clusters, icosahedral order and stability of quasicrystals - a view of metallurgy. *Sci. Technol. Adv. Mater.*, 9(1):013008, 2008.

R. Twarock. A tiling approach to virus capsid assembly explaining a structural puzzle in virology. *J. Theor. Biol.*, 226(4):477–482, 2004.

R. Twarock. Mathematical virology: a novel approach to the structure and assembly of viruses. *Phil. Trans. R. Soc.*, 364:3357–3373, 2006.

C. M. Wayman. *Introduction to the crystallography of martensite transformations.* Collier-Macmillan, 1964.

T. R. Welberry and B. Sing. Deformed Penrose tilings. *Phil. Mag.*, 87 (18–21):2877–2886, 2007.
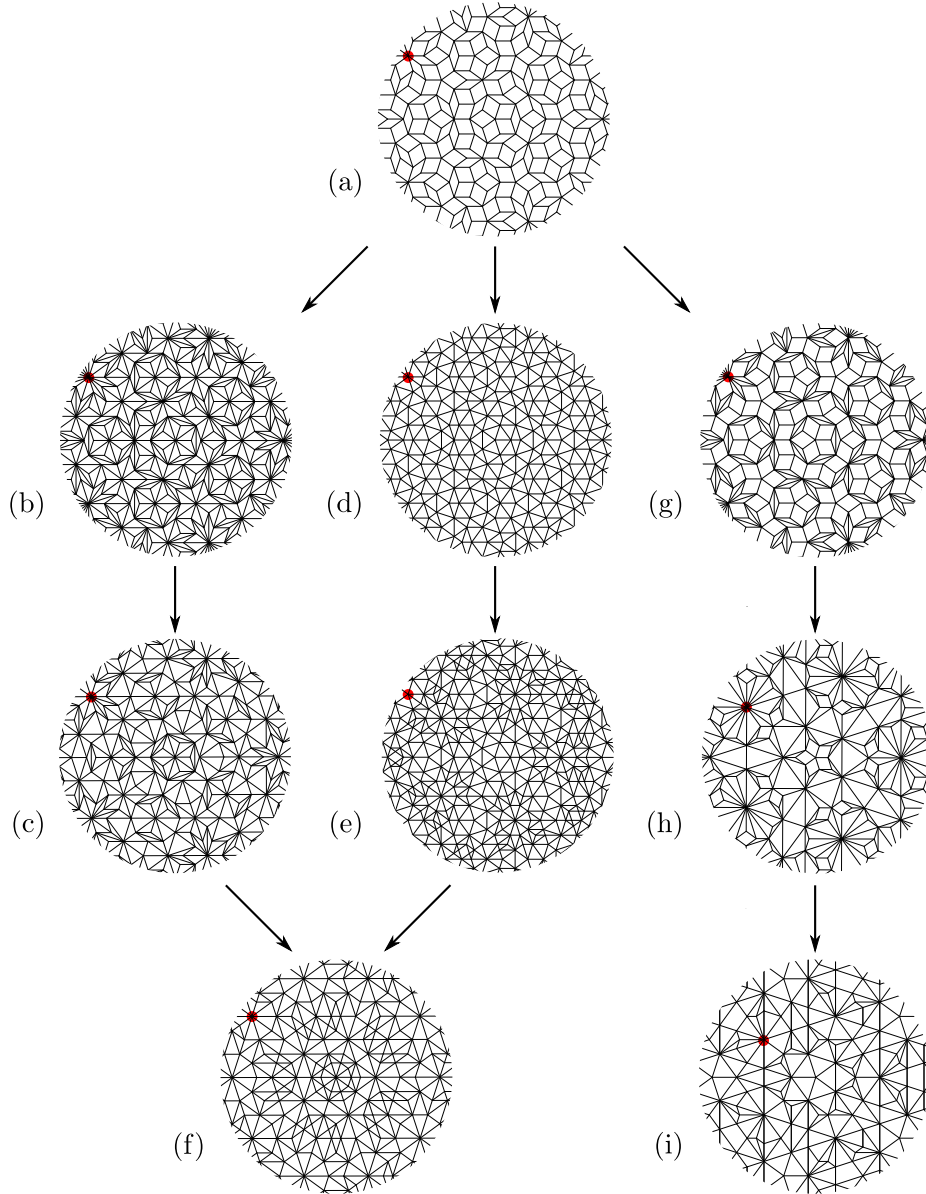
Figure 7: (a), (b), (c), (d), (e), (f): transition from the Penrose tiling (a) to the BCC tiling (f) via two pathways; (a), (b), (c), (f) is the path defined by (13), while (a), (d), (e), (f) is the path defined by (14). (a), (g), (h), (i): the transition from the Penrose tiling (a) to the FCC tiling (i) via the pathway defined by (15). The highlighted vertex corresponds to the 'same' lattice point and shows the relative scaling of the corresponding tilings.

24